Co-published from **Inorganic Letters**, 2014, 1(1), 9-22

Int. Res. Adv. 2014, 1(1), 22-35 Article

Integrated Research Advances / Inorganic Letters

Spectral analysis of μ-bridging coordination in triphenyl Sn(IV)-Al(III)-μ-oxoisopropoxide derivatives of alkylpyruvate aroylhydrazone : Interpretation of pharmacophore geometries

Rajni Johar,[1,3] Rajiv Kumar[1,2,*] and Ashok K Prasad[1]

[1]*Department of Chemistry, University of Delhi, Delhi 110007, India*
[2]*Department of Chemistry, SC, University of Delhi, New Delhi 110027, India*
[3]*Department of Chemistry, G.G.S. I.P. University, New Delhi, 110002, India*

Received on: 24-Dec-2013

ABSTRACT

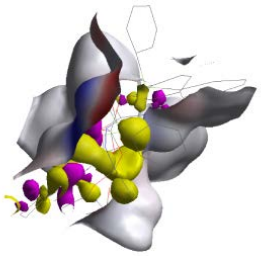
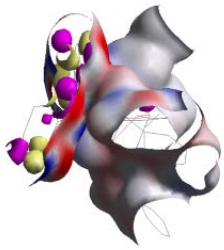

Triphenyl Sn(IV)-A(III)-µ-oxoisopropoxide derivatives having different (NOONO and OONO) backbones were obtained by the reaction of triphenyltin acetate and aluminium isopropoxide with corresponding ligand. Through variation of reaction stoichiometry, varieties of coordination compounds featuring µ-bridging coordination were synthesized. ^{119}Sn NMR spectra of $Ph_3SnOAl(OPr^i)L$ and $Ph_3SnOAl(L)_2$ exhibit a single resonance, in solution, which is a characteristic of four-coordinated triphenyl complex. There are quite close structural and architectural similarities between both series of complexes. Physicochemical analysis confirmed the formation of $Ph_3SnOAl(OPr^i)L$ and $Ph_3SnOAl(L)_2$ derivatives. Both the derivatives of triphenyl Sn(IV)-Al(III)-µ-oxoisopropoxide showed tetra- and penta- coordination of metal centres with distorted tetrahedral and distorted trigonal-bipyramidal geometries for Sn(IV) and Al(III) respectively. These central metal ions are capable of organizing surrounding atoms to achieve pharmacophore geometries by the variation of architectural elements of concerned ligands which are not readily and rapidly achieved by other means. Five complexes from each series were screened for their anti-fungal and antibacterial properties.

Keywords: organotin(IV) alkylpyruvate aroylhydrazones, ^{27}Al NMR, ^{119}Sn NMR and MS-spectroscopy

INTRODUCTION

Biomedical organometallic chemistry offers potential for the design of novel therapeutic and diagnostic agents. The mode of action of many medicinal organic compounds involves activation or biotransformation by metal ions, including metallo-enzymes. Many other mechanisms involve a direct or indirect effect of metal ion(s) on the activity of biomolecular

Dr. Rajiv Kumar
Email: chemistry_rajiv@hotmail.com
Tel: +91 9810742944; fax: +91 01234276530

Cite as: *Int. Res. Adv. 2014, 1(1), 22-35 or as Inorg. Lett. 2014, 1(1), 9-22.*

reactions. The dynamics of complexes are strongly controlled by the strength of the bonds between tin ion and functional donor atom. The ligands have steric and electronic properties by virtue of different donor atoms and so these properties can easily be tailored by replacement of different donor groups such as by reaction of amidine, ester and aroylhydrazone.[1] The presence of *p*-orbital's within donor subunits in ligand skeleton facilitates delocalization of negative charge across (-N=C=N-) or (-O-CH_2-O-) or –NH-CH=O backbone. This charge delocalization has an impact on variety of possible coordination modes with metals.[2,3] The ligands having oxygen, nitrogen or both donor set interact with metal centers through a variety of coordination modes including: (1) monodentate (amidate coordinates through either N or O) (2) bridging (N and O donors coordinate to same metal ions) and (3) chelating (where N- and O-donors coordinate to same metal ion) within ligands moiety. Thus possible coordination modes for such ligands vary by interacting with different approaches.[4,5] The fate of bound metals is of particular importance in $Ph_3SnOAl(OPr^i)L$ and $Ph_3SnOAl(L)_2$ because these has to achieve pharmacophore geometries for better molecular recognition in majority of biological activities.

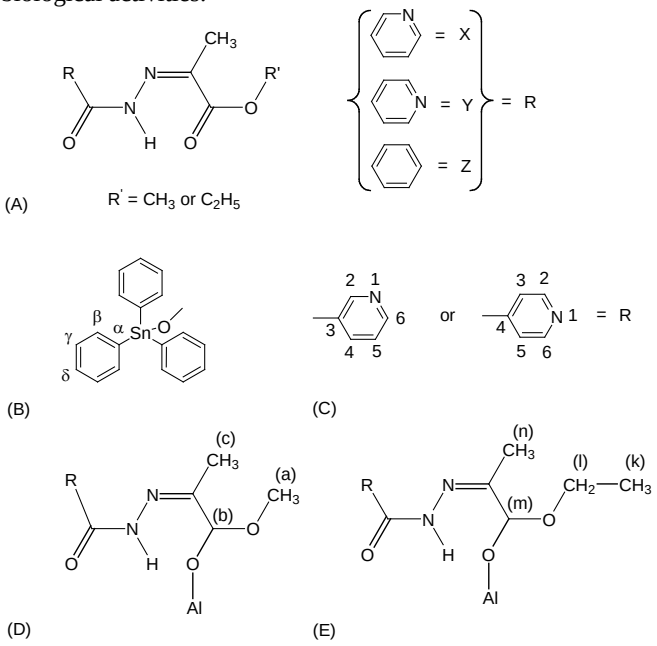

Figure. 1A-E. and ligands representations as (L_1-L_5). a-Ethylpyruvate nicotinoylhydrazone (L_1), b-Methylpyruvate nicotinoylhydrazone (L_2), c-Methylpyruvate isonicotinoylhydrazone (L_3), d-Ethylpyruvate isonicotinoylhydrazone (L_4), e-Ethylpyruvate benzoylhydrazone (L_5), where R = X = Nicotinoylhydrazone, R = Y = Isonicotinoylhydrazone, R = Z = Benzoylhydrazone. (1b) ^{1}H NMR representation for pyridine. (1c) ^{13}C-NMR representation. (1d and 1e) ^{13}C NMR representation of -CH_3 and -C_2H_5

The therapy for metal overload pathologies usually involves administration of suitable chelating agents to selectively remove metal from the body. The metal-based drugs play an important role in modern medicine as therapeutic and diagnostic agents.[6] Organotin compounds show a large spectrum of biological activities. Several organotin compounds have been found to be antineoplastic and antiviral agents, used commercially as bactericides, fungicides and acaricides. Some organotin compounds are potent biocides as they exhibited fungicidal activities. Triphenyltin acetate has been commercially marketed as a fungicide. The antifungal activities of organotin compounds have also been reported in literature.[7-9]

Owing to ever-growing importance of heterometallic alkoxides it was considered worthwhile to synthesize complexes of $Ph_3SnOAl(OPr^i)L$ and $Ph_3SnOAl(L)_2$ to gain an insight into their structural features with spectral techniques (IR, ^{1}H NMR, ^{13}C NMR, ^{27}Al NMR, ^{119}Sn NMR and MS) analysis and molecular modeling along-with their effectiveness as anti-microbial agents figure 1.A-E. Synthetic methodologies of such ligands can be designed by modifying ester or ether or thioether or amide linkages. There are ample opportunities to exploit the reactivity of triphenyltin ligand in the synthesis of unsaturated bimetallic complexes.

2 EXPERIMENTAL

2.1 Materials and Instruments

Precautions were taken to exclude moisture throughout the experimental procedure. Aluminium isopropoxide was prepared according to the reported method.[10-11] The solvents, alkyl pyruvate aroylhydrazone and triphenyltin acetate (Aldrich) were purified (re-crystallization) and dried prior to use.[12] Isopropyl acetate and isopropanol were estimated oxidimetrically while Al(III) and Sn(IV) were estimated gravimetrically.[13] Analytical data (CHN) of derivatives of alkyl pyruvate aroylhydrazone were obtained with Carlo-Ebra 1106 elemental analyzer. Melting points were determined on an electro-thermal melting point apparatus, model MP-D Mitamura Riken Kogyo, by capillary tube and are uncorrected. Infrared spectra were recorded as KBr pellets or then film on a FTIR Schimadzu spectrometer, over a range 4000-400 cm^{-1}. Mass spectra were recorded on a MAT 8500 Finnigan (Germany). ^{1}H NMR and ^{13}C NMR spectra were recorded on Bruker 300 with chemical shifts (δ) expressed in parts per million (ppm) relative to tetramethylsilane (TMS). ^{119}Sn-NMR spectra were obtained on a Bruker 250 ARX instrument with Me_4Sn as an external reference. The ^{27}Al NMR were recorded on a α-500 NMR spectrometer (JEOL) at a resonance frequency of 130.2 with a 10.5-μs (π/2) pulse length, an acquisition time of 5Hz was applied before the Fourier transformation. The chemical shift was relative to 0 ppm for the response of 10mM $AlCl_3$ solution (pH = 1) at the respective recording temperature.

2.2 Molecular Modeling

Correct sequence of atoms was obtained to get reasonable low energy molecular models to determine their molecular representation in three dimensions. Complications of molecular transformations could be explored using output obtained. An attempt to gain a better insight on molecular structure of $Ph_3SnOAl(OPri)L$ and $Ph_3SnOAl(L)_2$, geometric optimization and conformational analysis were performed using MM+2 force field. Potential energy of molecule was the sum of following terms: E = Estr + Eang + Etor + Evdw + Eoop + Eele. Where all E's represent energy values corresponds to given types of interaction. The subscripts str, ang, tor, vdw, oop and ele denote bond stretching, angular bonding, torsion deformation, van der waals interactions, out of plane bending and electronic interaction, respectively.[14] Thermodynamics data were DFT (Density Functional Theory). Calculations for the mechanism were carried out at Density Functional Theory (DFT) level with the hybrid functional B3LYP and isomerization at B3LYP/6-311G(d) level. The nature of all energy minima and transition states was confirmed via analytical frequency calculations. Transition states were further characterized by mimicking the unique imaginary frequency to confirm their relaxations to correct corresponding local minima. Quantum theory of atoms in molecules (QTAIM) analysis was employed.

2.3 Microbial assay

The free ligand and its organotin complex were tested against various bacterial strains with the agar well diffusion method. The antifungal activity against various fungi was also tested and the results are presented graphically.

2.4 Hanging drop method-antifungal activity

The concentration of the test compounds was 500 ppm used to study the antimicrobial activities on germination of fungal spores by the hanging drop method. The germination of the spores was observed under microscope after 8 hours of incubation at 30°C for incubation period 5-8 days. The percentage inhibition of spore germination was calculated as follows, % Inhibition of spore germination = Total number of germinated spore/ Total number of spore.

2.5 Agar well diffusion method-antibacterial activity

The antibacterial activity was determined using the agar well diffusion method. The well was dug in the media with a sterile borer and eight-hour bacterial inoculum containing ca. 104-106 colony-forming units (CFU)/ml was spread on the surface of the nutrient agar using a sterile cotton swab. The recommended con-centration of the best sample (2 mg/ml in DMSO) was introduced into respective wells. Other wells containing DMSO and the reference antibacterial drug served as negative and positive controls, respectively. The plates were incubated immediately at 37°C for 20 h. The activity was determined by measuring the diameter of the inhibition zone (in mm) showing complete inhibition. Growth inhibition was calculated with reference to the positive control.

3. Synthesis of Starting Compounds : $Ph_3SnOAl(OPr^i)_3$

3.1 Triphenyltinacetate (4.46 g, 10.9 mmol) and aluminium isopropoxide (2.22 g, 10.9 mmol) were refluxed in 1:1 molar ratio in xylene for 6 hrs in a fractionating column (1)

Isopropyl acetate formed during course of reaction was distilled continuously to the boiling point of xylene (139 °C). This was collected and estimated oxidimetrically to check the completion of the reaction.[15] Excess of solvent was removed under reduced pressure (40 °C /1mm). The product was redissolved in benzene and its slow evaporation resulted in pale amorphous solids (yield 98%).The μ-oxo compound was found to be soluble in common organic solvents such as $CHCl_3$ and C_6H_6, highly susceptible to hydrolysis and decomposed on heating (~170 °C).

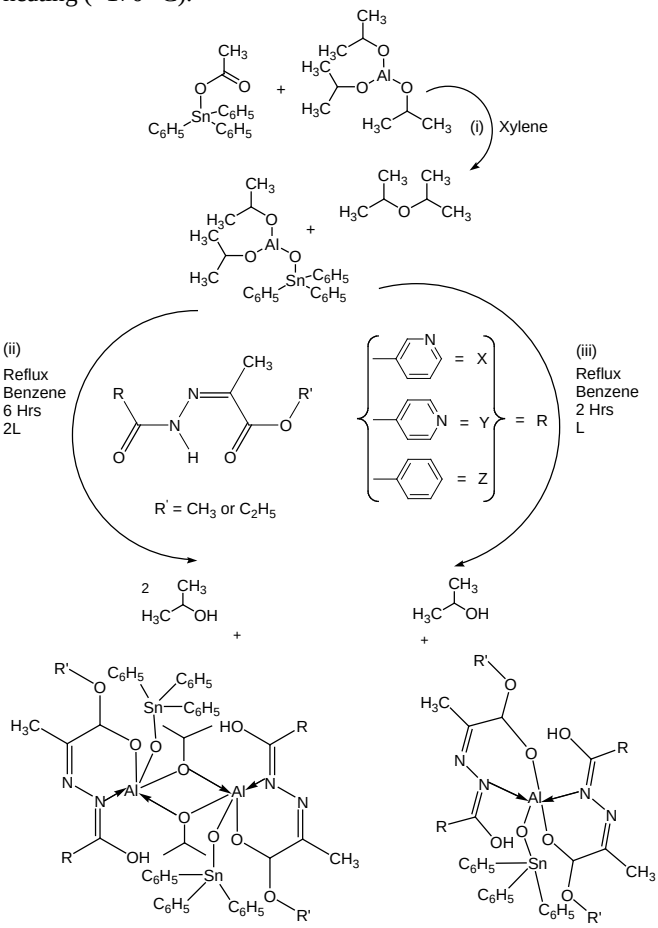

Figure. 2 Reaction and systematic pathways for the preparation of $Ph_3SnOAl(OPr^i)L$ and $Ph_3SnOAl(L)_2$

3.2 Reaction of $Ph_3SnOAl(OPr^i)_2$ with ethyl pyruvate benzoylhydrazone in 1:1 molar ratio (2)

To a clear solution of $Ph_3SnOAl(OPr^i)_2$ (0.214g 0.433 mmol) was added ethyl pyruvate benzoylhydrazone (L_5) (0.101g, 0.433 mmol) in 1:1 in ~60 ml benzene. The reaction contents were refluxed for 3 hrs in a fractionating column. The liberated isopropanol was collected at 72-78 °C as binary azeotrope of

isopropanol and benzene. The progress of the reaction was checked by estimating the isopropanol contents in the azeotrope by oxidimetric method. After the completion of the reaction, the excess solvent was removed under reduced pressure (40 °C /1mm). A brown product was obtained. The brown solid was washed with petroleum ether and dried under vacuum to get a light brown solid.

3.3 Reaction of $Ph_3SnOAl(OPr^i)_2$ with ethyl pyruvate benzoylhydrazone in 1:2 molar ratio (3)

Ethyl pyruvate benzoylhydrazone (L5) (0.198g, 0.846 mmol) was added to a clear solution of $Ph_3SnOAl(OPr^i)_2$ (0.214g, 0.423 mmol) in 1:2 in ~60 ml benzene. The reaction contents were refluxed for about 6 hrs in a fractionating column. The liberated isopropanol during the reaction was collected at 72-78 °C as binary azeotrope of isopropanol and benzene.

The progress of the reaction was checked by estimating the isopropanol contents in the azeotrope by oxidimetric method. After the completion of the reaction, the excess solvent was removed under reduced pressure (40 °C /1mm). Brown solid obtained was washed with petroleum ether and dried under vacuum to get a light brown solid. Scheme of the reaction is given in figure 2.

The reaction of $Ph_3SnOAl(OPr^i)_2$ with other alkyl pyruvate aroylhydrazones *viz* ethyl pyruvate nicotinoylhydrazone (L_1), methyl pyruvate nicotinoylhydrazone (L_2), methyl pyruvate isonicotinoylhydrazone (L_3) and ethyl pyruvate isonicotinoylhydrazone (L_4) in 1:1 and 1:2 molar ratio, and specified reaction mechanism for the complex formation for the ligand (L^4) was given and ethylpyruvate benzoylhydrazone (L5), were carried out by a similar procedure and their analytical data along with metal and liberated isopropanol estimations have been summarized in Table 1.

4. Results and Discussion

Complexes were colored, hygroscopic solids, stable in inert atmosphere. All the derivatives were found to be soluble in common organic solvents, moisture sensitive, and decomposed on heating. Their chemical analyses confirmed purity of derivatives of alkylpyruvate aroylhydrazone. Elemental analysis and mass spectra have good agreement with monomeric and diametric formulations of derivatives of alkylpyruvate aroylhydrazone and has been reported in table 1.

Table 1. Physiochemical analysis of $Ph_3SnOAl(OPr^i)L$ and $Ph_3SnOAl(L)_2$

S. No	Complexes g, mmol Formulae	Ligand g, mmol	Mass (m/z)	Molar Ratio	Elemental Analysis (%) Found (Calcd)				
					C	H	N	Sn	Al
C-1	$Ph_3SnOAl(OPr^i)L_1$ 0.300 (0.600) $C_{64}H_{72}Al_2N_6O_{10}Sn_2$	L_1 0.142 (0.600)	1378	1:1	55.01 (55.58)	5.10 (5.27)	5.99 (6.10)	17.30 (17.25)	3.80 (3.92)
C-2	$Ph_3SnOAl(L_1)_2$ 0.291 (0.580) $C_{40}H_{43}AlN_6O_7Sn$	L_1 0.276 (1.160)	866	1:2	55.23 (55.51)	4.67 (5.01)	9.45 (9.71)	13.81 (13.72)	3.02 (3.12)
C-3	$Ph_3SnOAl(OPr^i)L_2$ 0.332 (0.670) $C_{62}H_{68}Al_2N_6O_{10}Sn_2$	L_2 0.148 (0.670)	1350	1:1	55.12 (55.22)	4.78 (5.08)	6.11 (6.23)	17.82 (17.60)	4.02 (4.0)
C-4	$Ph_3SnOAl(L_2)_2$ 0.203 (0.410) $C_{38}H_{39}AlN_6O_7Sn$	L_2 0.181 (0.820)	838	1:2	54.12 (54.50)	4.50 (4.69)	10.00 (10.04)	14.33 (14.18)	3.17 (3.22)
C-5	$Ph_3SnOAl(OPr^i)L_3$ 0.137 (0.278) $C_{64}H_{72}Al_2N_6O_{10}Sn_2$	L_3 0.061 (0.278)	1378	1:1	55.23 (55.58)	5.11 (5.27)	5.78 (6.10)	18.24 (17.25)	4.05 (3.92)
C-6	$Ph_3SnOAl(L_3)_2$ 0.105 (0.212) $C_{38}H_{39}AlN_6O_7Sn$	L_3 0.094 (0.424)	838	1:2	54.34 (54.50)	4.34 (4.69)	9.66 (10.04)	14.74 (14.18)	3.05 (3.22)
C-7	$Ph_3SnOAl(OPr^i)L_4$ 0.220 (0.440) $C_{64}H_{72}Al_2N_6O_{10}Sn_2$	L_4 0.104 (0.440)	1378	1:1	55.67 (55.84)	5.10 (5.27)	6.00 (6.10)	16.25 (17.25)	3.55 (3.92)
C-8	$Ph_3SnOAl(L_4)_2$ 0.108 (0.218) $C_{40}H_{43}AlN_6O_7Sn$	L_4 0.102 (0.435)	866	1:2	55.01 (55.51)	4.90 (5.01)	9.65 (9.71)	14.25 (13.72)	3.15 (3.12)
C-9	$Ph_3SnOAl(OPr^i)L_5$ 0.214 (0.433) $C_{66}H_{74}Al_2N_4O_{10}Sn_2$	L_5 0.101 (0.433)	1376	1:1	57.11 (57.66)	5.32 (5.43)	3.98 (4.08)	17.36 (17.27)	3.83 (3.93)
C-10	$Ph_3SnOAl(L_5)_2$ 0.210 (0.423) $C_{42}H_{45}AlN_4O_7Sn$	L_5 0.198 (0.846)	864	1:2	58.22 (58.42)	3.00 (3.12)	6.32 (6.49)	13.77 (13.75)	3.13 (3.12)

Beside physiochemical analysis, spectral techniques (IR, ^{1}H NMR, ^{13}C NMR, ^{27}Al NMR, ^{119}Sn NMR and MS) analysis and molecular modeling were also summarized and presented below.

4.1 Infrared spectra

In order to clarify the mode of coordination between donor atoms i.e. N, O and metals centres i.e. Sn(IV) and Al(III), IR spectra and far infrared regions were reported in the 4000-400 cm^{-1}. The assignment of IR bands of synthesized compounds was determined by comparison with IR spectra of ligands. The most important bands were presented with their assign as per their relative groups in table 2. Some of these characteristics bands have been discussed below with their relative peaks assignments and values. OAc groups showed sharp bands at 1710-1705 cm^{-1} in Ph_3SnOAc and these bands were absent in IR spectra of $Ph_3SnOAl(OPr^i)_2$ indicating complete removal of acetyl group after changing the ratio of reactants. Bands assignable to *gem*-dimethyl moiety of isopropoxy groups were observed at 1373-1362 cm^{-1}. Medium intense bands at 1125-1115 cm^{-1} and 1070-1052 cm^{-1} were present due to the terminal and bridging isopropoxy groups as expected in IR spectra of $Ph_3SnOAl(OPr^i)_2$ derivatives.[16]

Moreover, strong to medium stretching frequencies appeared at 972-960 cm^{-1} corresponding to υ(C-O) of isopropoxy groups.[17] The bands at 1710-1705 cm^{-1} due to the presence of υ(>C=O) groups suggested non-coordination of one of carbonyl groups. IR spectra of $Ph_3SnOAl(OPr^i)(L)$ and $Ph_3SnOAl(L)_2$ showed absence of bands in the range of 3280 to 3160 cm^{-1} confirming deprotonation of -NH groups. Bands at 1520-1515 cm^{-1} assigned to amide (II) were found to be absent in complexes. Instead of these bands, medium bands at 1665-1660 cm^{-1} were detected corresponding to υ(C=N) group confirming the formation of conjugate systems >C=N-N=C<.[18] A downward shift ~20 cm-1 was observed for amide (II) due to the coordination through azomethine nitrogen and thereby, suggesting bidentate nature of ligands.

The bands in the region 550-510 cm^{-1} and 450-420 cm^{-1} were observed due to the formation of new metal-donor bonds i.e. υ(Sn-C) and υ(Sn-O), during complexes formation.[19] A number of bands were observed in the regions 700-400 cm^{-1} due to M-O stretching vibrations (because of μ-oxo bridge formation) in derivatives of $Ph_3SnOAl(OPr^i)_2$.[20] The bands related to phenyl groups occurred at their usual positions.

4.2 ^{1}H NMR Spectra

The ^{1}H-NMR integration values were completely consistent with the formulation of products and reported in table 3. The signals were assigned by their peak multiplicity, intensity pattern, integration, and satellites. ^{1}H NMR spectrum of

Table 2. Infrared spectral bands (cm^{-1}) of $Ph_3SnOAl(OPr^i)L$ and $Ph_3SnOAl(L)_2$

OMCs	υ_{OH}	$\upsilon_{Py-N=}$	υ_{C-O}	$\upsilon_{C=N}$	$\upsilon_{C-N=}$	υ_{Ph}	-O<CH3	-O-	υ_{Sn-C}	υ_{Sn-O}	υ_{Al-O}	$\upsilon_{Al\rightarrow N}$	$\upsilon_{Al\rightarrow O}$
$Ph_3SnOAl(OPr^i)(L_1)$	3401	1725	1710s	1660	1520s	1625	1373	1052	550	450	721, 560	590	350
$Ph_3SnOAl(L_1)_2$	3400	1720	1705s	1661	1520s	1621	1370	1055	540	430	724, 567	590	321
$Ph_3SnOAl(OPr^i)(L_2)$	3402	1715	1708s	1660	1516s	1624	1364	1068	515	420	725, 566	590	341
$Ph_3SnOAl(L_2)_2$	3406	1715	1710s	1661	1520s	1627	1362	1070	510	450	723, 565	581	349
$Ph_3SnOAl(OPr^i)(L_3)$	3408	1716	1705s	1660s	1517s	1620	1362	1060	544	450	723, 567	584	345
$Ph_3SnOAl(L_3)_2$	3409	1720	1710s	1660s	1518s	1629	1363	1069	547	422	720, 565	586	346
$Ph_3SnOAl(OPr^i)(L_4)$	3410	1722	1705s	1663s	1520s	1622	1370	1066	594	433	720, 564	589	345
$Ph_3SnOAl(L_4)_2$	3403	1722	1709s	1660s	1515s	1622	1370	1061	540	429	722, 564	582	347
$Ph_3SnOAl(OPr^i)(L_5)$	3405	1724	1709s	1662	1516s	1622	1365	1069	550	441	722, 564	589	341
$Ph_3SnOAl(L_5)_2$	3407	1720	1706s	1665	1515s	1624	1373	1066	522	449	722, 562	589	246

Table 3. ^{1}H NMR spectral bands (δ) of $Ph_3SnOAl(OPri)L$ and $Ph_3SnOAl(L)_2$

Complexes	Sn-Phenyl	[nicotinoyl or isonicotinoyl] R = X, Y, Z	O-(OC)-R′; R′ = CH_3, C_2H_5	(Pr^i) or [-O-CH-(CH_3)$_2$] -CH_3
$Ph_3SnOAl(OPr^i)(L_1)$	7.93-7.81, *J* [8.5 Hz] (m, 12H, Sn-Ph_O); 7.41-7.34, *J* [4.0 Hz] (m, 12H, Sn-Ph_m); 7.21-7.19, *J* [1.0 Hz] (m, 18H, Sn-Ph_p)	8.85 (s, 2H, H_2), 7.13 (d, J = 8.1 Hz, 2H, H_4), 7.44 (td, J = 7.6, Hz, 2H, H_5), 8.69 (dd, J = 6.7, Hz, 2H, H_6)	4.25 (q, 4H, H_l), J [7 Hz], 1.69 (t, 6H, H_k), J [7 Hz], 1.15 (s, 2H, H_m)	4.23-4.11 (m, 2H, H_{Pri}) [J = 11.0 Hz], 2.33 (dd, 12H, H_{Pri}) [J = 3.0 Hz], 1.3 (s, 6H, H_n)
$Ph_3SnOAl(L_1)_2$	8.00-7.87, *J* [8.0 Hz] (m, 12H, Sn-Ph_O); 7.51-7.49, *J* [3.0 Hz] (m, 12H, Sn-Ph_m); 7.40-7.33, *J* [1.8 Hz] (m, 18H, Sn-Ph_p)	8.81 (s, 2H, H_2), 7.68 (d, J = 8.1 Hz, 2H, H_4), 7.40 (td, J = 7.6, Hz, 2H, H_5), 8.77 (dd, J = 6.7, Hz, 2H, H_6)	4.29 (q, 4H, H_l), J [7 Hz], 1.68 (t, 6H, H_k), J [7 Hz], 1.16 (s, 2H, H_m)	1.2 (s, 6H, H_c)
$Ph_3SnOAl(OPr^i)(L_2)$	7.90-7.81, *J* [7.0 Hz] (m, 12H, Sn-Ph_O); 7.60-7.52, *J* [4.2 Hz] (m, 12H, Sn-Ph_m); 7.50-7.46, *J* [2.0 Hz] (m, 18H, Sn-Ph_p)	8.81 (s, 2H, H_2), 7.60 (d, J = 8.1 Hz, 2H, H_4),7.38 (td, J = 7.6, Hz, 2H, H_5), 8.71 (dd, J = 6.7, Hz, 2H, H_6)	3.9 (s, 3H, H_a) 1.13 (s, 2H, H_b)	4.21-4.13 (m, 2H, H_{Pri}) [J = 10.2 Hz], 2.28 (d, 12H, H_{Pri}) [J = 3.2.0 Hz],1.3 (s, 6H, H_n)
$Ph_3SnOAl(L_2)_2$	7.80-8.72, *J* [8.0 Hz] (m, 12H, Sn-Ph_O); 7.54-7.47, *J* [4.0 Hz] (m, 12H, Sn-Ph_m); 7.40-7.33, *J* [2.0 Hz] (m, 18H, Sn-Ph_p)	8.91 (d, 2H, H_2), 7.80 (d, J = 7.9 Hz, 2H, H_4), 7.21 (td, J = 8.0, 1.2 Hz, 2H, H_5), 8.70 (dd, J = 6.6, 5.7 Hz, 2H, H_6)	3.9 (s, 3H, H_a) 1.12 (s, 2H, H_b)	1.2 (s, 6H, H_c)
$Ph_3SnOAl(OPr^i)(L_3)$	8.00-7.91, *J* [7.5 Hz] (m, 12H, Sn-Ph_O); 7.61-7.58, *J* [2.5 Hz] (m, 12H, Sn-Ph_m); 7.30-7.26, *J* [2.0 Hz] (m, 18H, Sn-Ph_p)	8.79 (d, 4H, J = 5.0 Hz, $H_{2,6}$), 7.69 (dd, J = 6.7, Hz, 4H, $H_{3,5}$)	3.8 (s, 3H, H_a) 1.16 (s, 2H, H_b)	4.21-4.12 (m, 2H, H_{Pri}) [J = 11.1 Hz], 2.18 (d, 12H, H_{Pri}) [J = .1 Hz],1.3 (s, 6H, H_n)
$Ph_3SnOAl(L_3)_2$	8.00-7.89, *J* [8.0 Hz] (m, 12H, Sn-Ph_O); 7.43-7.38, *J* [3.5 Hz] (m, 12H, Sn-Ph_m); 7.20-7.18, *J* [1.2 Hz]; (m, 18H, Sn-Ph_p)	8.80 (d, 4H, J = 5.0 Hz, $H_{2,6}$), 7.72 (dd, J = 6.7, Hz, 4H, $H_{3,5}$)	3.7 (s, 3H, H_a) 1.13 (s, 2H, H_b)	1.2 (s, 6H, H_c)
$Ph_3SnOAl(OPr^i)(L_4)$	7.90-7.83, *J* [7.5 Hz] (m, 12H, Sn-Ph_O); 7.43-7.39, *J* [3.0Hz] (m, 12H, Sn-Ph_m); 7.20-7.17, *J* [1.5 Hz] (m, 18H, Sn-Ph_p)	8.84 (d, 2H, J = 5.0 Hz, $H_{2,6}$), 7.72 (dd, J = 6.7, Hz, 2H, $H_{3,5}$)	4.28 (q, 4H, H_l), J [7 Hz], 1.61 (t, 6H, H_k), J [7 Hz], 1.14 (s, 2H, H_m)	4.10-4.05 (m, 2H, H_{Pri}) [J = 11.0 Hz], 2.28 (d, 12H, H_{Pri}) [J = 2.8 Hz],1.3 (s, 6H, H_n)
$Ph_3SnOAl(L_4)_2$	8.0-7.91, *J* [7.8 Hz] (m, 12H, Sn-Ph_O); 7.61-7.58, *J* [2.5 Hz] (m, 12H, Sn-Ph_m); 7.40-7.37, *J* [1.5 Hz] (m, 18H, Sn-Ph_p	8.81 (d, 4H, J = 5.0 Hz, $H_{2,6}$), 7.77 (dd, J = 6.7, Hz, 4H, $H_{3,5}$)	4.25 (q, 4H, H_l), J [7 Hz], 1.60 (t, 6H, H_k), J [7 Hz], 1.14 (s, 2H, H_m)	1.2 (s, 6H, H_c)
$Ph_3SnOAl(OPr^i)(L_5)$	7.90-7.81, *J* [7.2 Hz] (m, 12H, Sn-Ph_O); 7.41-7.34, *J* [4.5 Hz] (m, 12H, Sn-Ph_m); 7.20-7.19, *J* [0.8 Hz] (m, 18H, Sn-Ph_p)	7.30-7.14 (m, 5H, Ar) *J* [6.5 Hz]	4.29 (q, 4H, H_l), J [7 Hz], 1.65 (t, 6H, H_k), J [7 Hz], 1.16 (s, 2H, H_m)	4.10-4.02 (m, 2H, H_{Pri}) [J = 10.8 Hz], 2.27 (d, 12H, H_{Pri}) [J = 3.4 Hz],1.3 (s, 6H, H_n)
$Ph_3SnOAl(L_5)_2$	7.80-7.73, *J* [7.2 Hz] (m, 12H, Sn-Ph_O); 7.45-7.39, *J* [4.0 Hz] (m, 12H, Sn-Ph_m); 7.30-7.26, *J* [2.0 Hz] (m, 18H, Sn-Ph_p)	7.28-7.14 (m, 5H, Ar) *J* [6.5 Hz]	4.31 (q, 4H, H_l), J [7 Hz], 1.61 (t, 6H, H_k), J [7 Hz], 1.16 (s, 2H, H_m)	1.2 (s, 6H, H_c)

$Ph_3SnOAl(OPr^i)L_5$ and $Ph_3SnOAl(L_5)_2$ showed a multiplet centered at δ 7.30-7.14 due to phenyl protons. Disappearance of signal at δ 10.8-10.7 in complexes confirmed deprotonation of >NH proton. A multiplet and doublet centered at δ 4.23-4.02 ppm and 2.33-2.18 ppm corresponding to methylene and methyl protons of overlapping bridging and terminal isopropoxy (Pr^i).[21]

In ^{1}H-NMR spectra of reported complexes, migration of proton between -NH- and >C=O groups occurred, such exchange of protons bring equilibrium in compounds moiety. This helped to explain the replacement of proton from -NH- to carboxylic group and showed hydroxyl character which influence the organotin(IV) bonding in the moiety. The -NH- signal almost changed, indicating the involvement of thus group in inter/intramolecular hydrogen bonding or in bonding and H_b] attached to azomethine group were observed as a singlet at 1.3-1.2 ppm.[22]

4.3 ^{13}C NMR Spectra

Participation of alcoholic -OH/alcoholate -O$^-$ groups in coordination was mostly determined by their steric arrangement within the molecule. MM force field calculations performed for all Sn(IV) and Al(III) complexes showing tetra and penta coordination of ligand. Chelation of ligand was less favoured,

Table 4. ^{13}C NMR spectral bands (δ) of $Ph_3SnOAl(OPr^i)L$ and $Ph_3SnOAl(L)_2$

Complexes	Ester	Amide	>C=N-	Me-C=N-	-O-Me	-O-Et	Sn-(C_6H_5)$_3$; ($^{n}J(^{13}C-^{119/117}Sn$, Hz))
$Ph_3SnOAl(OPr^i)$ (L_1)	164.9, 173.2	145.1, 150.2	139.6	13.2	-	62.5 18.1	(C-α) 132.2 *J* [610, 612.2], (C-β) 125.0 *J* [59], (C-γ) 122.3 *J* [63], (C-δ) 113.5, *J* [16], ppm
$Ph_3SnOAl(L_1)_2$	165.1, 172.8	145.7, 150.7	139.5	13.1	-	62.7 18.3	(C-α) 133.1 *J* [619, 629.1], (C-β) 121.0 *J* [51], (C-γ) 120.3 *J* [61], (C-δ) 119.5, *J* [17], ppm
$Ph_3SnOAl(OPr^i)$ (L_2)	164.9, 173.1	145.3, 150.3	139.5	13.1	52.6	-	(C-α) 134.1 *J* [613, 624.0], (C-β) 125.1 *J* [64], (C-γ) 121.3 *J* [60], (C-δ) 119.5, *J* [16], ppm
$Ph_3SnOAl(L_2)_2$	164.9, 173.1	145.3, 150.3	139.5	13.1	52.6	-	(C-α) 135.0 *J* [626.1, 611.0], (C-β) 126.9 *J* [58], (C-γ) 124.1 *J* [60], (C-δ) 118.2, *J* [17], ppm
$Ph_3SnOAl(OPr^i)$ (L_3)	164.8, 172.5	145.2, 151.2	139.7	13.1	52.8	-	(C-α) 137.1 *J* [615, 610.1], (C-β) 127.1 *J* [64], (C-γ) 126.1 *J* [60], (C-δ) 118.5, *J* [15], ppm
$Ph_3SnOAl(L_3)_2$	164.9, 173.1	145.1, 150.3	139.8	13.0	52.7	-	(C-α) 137.2 *J* [621, 616.3], (C-β) 129.0 *J* [63], (C-γ) 126.3 *J* [64], (C-δ) 1121.5, *J* [17], ppm
$Ph_3SnOAl(OPr^i)$ (L_4)	164.7, 172.9	144.9, 150.9	138.9	13.1	-	62.4 18.3	(C-α) 138.4 *J* [631, 619.7], (C-β) 129.2 *J* [61], (C-γ) 126.3 *J* [61], (C-δ) 121.15, *J* [15], ppm
$Ph_3SnOAl(L_4)_2$	164.6, 173.5	144.7, 150.7	138.8	13.2	-	62.7 18.4	(C-α) 136.5 *J* [631, 617.3], (C-β) 131.0 *J* [58], (C-γ) 129.2 *J* [62], (C-δ) 120.3, *J* [18], ppm
$Ph_3SnOAl(OPr^i)$ (L_5)	164.1, 173.6	144.7, 150.8	139.5	13.1	-	62.8 18.1	(C-α) 136.7 *J* [619, 615.7], (C-β) 131.5 *J* [63], (C-γ) 1125.3 *J* [53], (C-δ) 122.5, *J* [19], ppm
$Ph_3SnOAl(L_5)_2$	164.2, 173.8	144.9, 150.2	139.3	13.1	-	62.9 18.1	(C-α) 134.4 *J* [622, 610], (C-β) 131.0 *J* [56], (C-γ) 127.3 *J* [61], (C-δ) 122.2, *J* [17], ppm

to organotin.

All the protons present in synthesized compounds were identified. The CH_3-O- and CH_3-CH_2-O- [H_a and $H_{k,l}$] protons of $Ph_3SnOAl(OPr^i)L$ and $Ph_3SnOAl(L)_2$ appeared as sharp singlet with well-defined satellites at 4.31-4.25 (q, 4H) and 1.69-1.60 (t, 6H) respectively. The protons of triphenyltin(IV) derivatives mostly showed a complex patter around δ 8.0-7.91 (m, 12H, Sn-Ph_O), 7.61-7.34, (m, 12H, Sn-Ph_m) and 7.40-7.19 (m, 18H, Sn-Ph_p). The methylene protons -CH- of Al(III) moieties exhibited somewhat different behavior compared with -CH_2- groups. Protons of pyridine moieties appeared at 8.91-7.13 ppm and 8.84-769 ppm for nicotinoylhydrazones and isonicotinoylhydrazones respectively. The methyl protons [H_n their steric energy level was about 20-30% higher and this increase was probably not counterbalanced by the bond energy of the additional Al-OH interaction.

The ^{13}C-NMR spectra of Sn-Ph skeletons $^{n}J(^{13}C-^{119/117}Sn$, Hz) displayed (C-α) 138.4-132.2 *J* [631.0, 619.1], (C-β) 131.5-121.0 *J* [64-51], (C-γ) 129.2-120.3 *J* [63-53], (C-δ) 122.2-113.5, *J* [18-15], ppm as expected for triphenyltin(IV) complexes and presented a similar picture: the signals ascribed to C(1), C(2) and C(5) were shifted and broadened as compared with the signals of L_1 to L_5 itself, whereas the signals corresponding to C(3) and C(4) were much affected. This selective line broadening and chemical shift changes some of the signals indicated that concerned protons and carbon atoms might be close to functional groups involved in Al(III)

coordination, namely -OH/-NH- groups of C(5) were assumed to participate in metal chelation. Participation of -OH/-NH- groups in the coordination was mostly determined by steric arrangement.

Peaks at δ 26.2 and δ 27.3 assigned to methyl carbons of terminal and inter molecularly bridged isopropoxy moieties and signals at δ 59.6 assigned to methine carbons of isopropoxy groups were absent in 1:2 derivatives which confirmed complete removal of isopropoxy group. Isopropoxy moiety resonated at δ 27.6 and δ 62.7 in 1:1 derivative for intermolecular bridged ends.[23] Resonance observed between δ 127.5-109.3 confirmed pyridine nucleus for ether and methyl nicotinoylhydrazones and isonicotinoylhydrazones derivatives respectively. ^{1}H-NMR spectra data of alkyl pyruvate aroylhydrazones of Ph3SnOAl$(OPr^{i})_2$ has been presented in table 4. Two set of amide and ester groups respectively appeared at δ 150.9-144.7 and δ 173.8-164.1. Another set of signals showed it presence at δ 52.8-52.6 for methoxy carbon whereas signals of ethoxy carbons found at δ 62.9-62.4 and δ 18.4, δ 18.1. Aryl and olefin carbons absorbed at δ 139.9-139.3 and δ 127.5-113.1 respectively.[24]

4.4 ^{119}Sn NMR Spectra

^{119}Sn NMR Spectra of $Ph_3SnOAl(OPr^{i})L$ and $Ph_3SnOAl(L)_2$ showed a sharp peak, with a chemical shift of δ -81.2 to -79.9 and δ -107 to -106 respectively. The ^{119}Sn NMR spectra of $Ph_3SnOAl(OPr^{i})L$ and $Ph_3SnOAl(L)_2$ exhibited a single resonance in solution, which was characteristic of four-coordinated triphenyl compounds. Nevertheless, a tetrahedral arrangement of Sn(IV) for $Ph_3SnOAl(OPr^{i})L$ and $Ph_3SnOAl(L)_2$ was proposed in solution because there are quite close structural similarities between $Ph_3SnOAl(OPr^{i})L$ and $Ph_3SnOAl(L)_2$. The values were indicative of a higher coordination number, where a four-coordinated environment around tin atom was suggested.[25]

In the case of $Ph_3SnOAl(OPr^{i})L$ two slightly different magnetic environments for tin were explained due to -μ-bridging. Thus, on the basis of above spectral studies in solution, it is clear that ligands (L_1 to L_5) behaves as a bidentate ligand coordinating through (O)/(N) to tin. In contrast, in the solid state, a higher coordination number was observed for $Ph_3SnOAl(OPr^{i})L$ where all ligands behaved differently.

The value of δ^{119}Sn defined region of various coordination numbers of tin. The results have been listed in table 5. In all complexes, ^{119}Sn spectra showed a sharp singlet indicting the formation of single species. ^{119}Sn chemical shift δ(^{119}Sn) of organotin compounds covered a range of over 600 ppm and were quoted relative to tetramethyltin with downfield shifts from reference compound having a negative sign. As electron releasing power of alkyl groups increased towards tin atom, the peaks become progressively more shielded and δ(^{119}Sn) values moved to a higher field. These values were also dependent upon the nature of ligand donor capabilities, generally move to a lower field as electronegativity of latter increased. ^{119}Sn chemical shift increased the coordination number of tin from 4 to 5, 6, or 7 usually produces a large up-field shift of δ(^{119}Sn). These values were strongly dependent upon the nature and orientation of organic groups bonded to tin.[26-27] The shifts observed in complexes can be explained quantitatively in terms of an increase in electron density on tin atom as coordination number increases. As increase in coordination number was accompanied by an appropriate upfield shift. It was generally accepted that compounds with a specific geometry around tin atom produces shifts in moderately well-defined ranges.

4.5 ^{27}Al NMR spectra

^{27}Al NMR spectra of $Ph_3SnOAl(L)_2$ showed a singlet at δ 41.4-39.5 ppm indicating trigonal bipyramidal geometry around Al atom surrounding by 3(O) atoms and 2(N) atoms whereas, alkylpyruvate aroylhydrazone derivatives of $Ph_3SnOAl(OPr^{i})_2$ showed singlet at δ 70.2-70.0 ppm indicating trigonal bipyramidal geometry around Al atom surrounding by 4(O) atoms and 1(N) atoms.[28] This was due to the replacement of both isopropoxy groups on Al atom. Observed assignments of relative peaks have been summarized in table 5.

As in related carboxylate or ether systems, the assignment of coordination numbers to Al centers in some compounds was controversial. As a general trend, it has been shown that, the overall coordination number at Al atom decreases with increasing in number of organic substituents at Al atom. This phenomenon was usually achieved by increased asymmetry in mode of coordination of O and N-donor ligands. Coordination of different alkyl groups with O-donor ligands does not change coordination geometry of triorganotin complexes showing polymeric structure with trigonal bipyramidal geometry.

Table 5. ^{27}Al and ^{119}Sn NMR spectral bands (δ) of $Ph_3SnOAl(OPr^{i})L$ and $Ph_3SnOAl(L)_2$

Complexes	δ(Al)	δ(Sn)
$Ph_3SnOAl(OPr^{i})(L_1)$	70.1	-801
$Ph_3SnOAl(L_1)_2$	39.6	-106.1
$Ph_3SnOAl(OPr^{i})(L_2)$	70.2	-81.1
$Ph_3SnOAl(L_2)_2$	40.5	-106
$Ph_3SnOAl(OPr^{i})(L_3)$	70.1	-80.2
$Ph_3SnOAl(L_3)_2$	39.5	-106.1
$Ph_3SnOAl(OPr^{i})(L_4)$	70.0	-79.9
$Ph_3SnOAl(L_4)_2$	41.4	-107.0
$Ph_3SnOAl(OPr^{i})(L_5)$	70.1	-80.0
$Ph_3SnOAl(L_5)_2$	40.1	-106.0

As seen, the coordination geometry around Al(III) atom was penta-coordinated distorted trigonal bipyramidal with two R groups attached to tin and S(1)/(S2) occupying equatorial positions while O(1) and N(2)/N(1) occupy apical position. In this way, ligand behaved as bidentate and chelated tin by means of O.[29]

4.6 TOF-MS Spectra

In mass spectra of Sn(IV) and Al(III) compounds, molecular ion peaks corresponding to various fragments (ligand or fragments of the ligand with metal or metal + ligand) were

observed according to their molecular formula. In initial peaks, it could be easily observed that used ligand degraded and broke down into various fragments such as [$C_8H_{15}NO_5$] showing a molecular ion peak at 196 (m/z values) with low intensity and have many more fragments like this. Due to degradation, another fragment pattern appeared at 163/196/206 (m/z) Sn(IV) and Al(III) compounds) with different intensity and a very strong peak was also observed at 263/264/4 with 100% intensity separately, which had a correlation with fragmentation patterns of Sn(IV) L_1 to L_5 and Al(III) compounds respectively.[30] The obtained results represented the degradation and demetallation patterns for Sn(IV) and Al(III) compounds.

In TOF-mass spectra of Sn(IV) and Al(III), initial fragmentation patterns showed mass loss of double bonded nitrogen fragments >N-C=NH from parent molecule at 690 and 687 (ligand fragments + metal) respectively. Mass degradation patterns provided important information regarding fragmentations in presence of isotropic ratio corresponding to metals i.e. Sn(IV) and Al(III) along with ligand fragments. In mass spectra of Sn(IV) and Al(III), molecular ion peaks (ligand + metal) were observed at 730 and 824 (m/z) respectively representing final molecular ion peak (m/z) presented in Table 1. In triorganotin(IV) carboxylates, primary fragmentation was due to the loss of R group and same was true for diorganotin(IV) derivatives. However, the secondary and tertiary decomposition was also followed by the loss of R group in triorganotin(IV) derivatives, while diorganotin(IV) derivatives manifest slightly different patterns of fragmentation.

On the basis of above mentioned results, following suggested geometrical arrangement of $Ph_3SnOAl(OPri)L$ and $Ph_3SnOAl(L)_2$ complexes were presented in figure 3(a) and (b) respectively.

5. Molecular modeling of $Ph_3SnOAl(OPr^i)L$ and $Ph_3SnOAl(L)_2$

Molecular coordinates depend on hybridization of an atom and mode of bonding as a standard to judge specific interactions in topologies of molecules.[31] If deviations in distances, angles or torsion were evidenced, specific electronic interactions should perhaps be pursued. In order to ascertain structural and geometrical features of $Ph_3SnOAl(OPr^i)(L)$ and $Ph_3SnOAl(L)_2$ derivatives through spectral evidences, coordination capabilities of metal centres confirmed molecular geometries.

The molecular structures of $Ph_3SnOAl(OPr^i)(L)$ and $Ph_3SnOAl(L)_2$ showed that Sn(IV) metal center of an infinite one-dimensional chain, having four-coordinated distorted tetrahedron geometry. In the case of $Ph_3SnOAl(OPr^i)(L)$, repeating unit comprised two different moieties with the planes of bridging ligands having twisted architecture. The overall geometry of Al(III) was a distorted trigonal-bipyramidal in which equatorial plane was formed from alkyl or phenyl groups of triorganotin moieties, while carboxyl oxygen and imidazole nitrogen occupied axial positions. Distortion from the distorted trigonal-bipyramidal geometry for $Ph_3SnOAl(OPr^i)(L)$ and $Ph_3SnOAl(L)_2$ can be observed from rather long =N-N= distances (2.163 to 2.412Å) and small deviations (172.61 to 178.4 Å) towards ideal 180 Å for apical positions.

The particular characteristics of these systems facilitated by coordination of an imidazole –N= atom to Sn(IV) instead of carbonylic moiety, which showed that coordination to –N= was favored rather than coordination to -O- atom. Bond angles of $Ph_3SnOAl(OPr^i)L_5$ and $Ph_3SnOAl(L_5)_2$ were presented in table 6 and 7. Bond angles between metal and donor atoms in moiety were somewhat selected upon coordination; bonds angles among Sn(25)-O(44)-Al(45) was 129.6, consequence of bonding were quite near to distorted trigonal-bipyramidal geometry.

Table 6. Bond Angles of $Ph_3SnOAl(OPr^i)L_5$

S. No	Geometrical sequencing of atoms	Bond Angle (º)	S. No.	Atoms numbering and their location	Bond Angle (º)
1.	C(32)-Sn(25)-C(104)	109.1	8.	C(26)-Sn(90)-O(109)	133.4
2.	C(32)-Sn(25)-C(137)	107.6	9.	C(91)-Sn(90)-O(109)	116.5
3.	Sn(25)-O(44)-Al(45)	129.6	10	C(97)-Sn(90)-O(109)	114.7
4.	O(18)-Al(45)-O(44)	136.5	11	Sn(90)-C(91)-C(92)	124.9
5.	O(18)-Al(45)-O(46)	115.1	12	C(26)-Sn(90)-O(109)	133.4
6.	Al(45)-O(47)-Al(110)	131.3	13	O(47)-Al(110)-O(109)	107.5
7.	N(74)-N(73)-Al(110)	110.7	14	Sn(25)-C(137)-C(161)	131.5

It indicated that all the active groups taking part in coordination had longer bonds than already existing >C=N- linkages of ligand moiety. Coordination significantly shortens as for 1.97 [Å] as compared to 1.96 [Å] for O(44)-Sn(25). This was because of bond lengths in ligands between donor atoms probably gets affected due to the presence of nitrogen in azo linkage (-N=N-). There was a large variation in N(18)-Al(45)-N(53) bond lengths on complexation and becomes slightly longer as the coordination took place via N atom of -N=N-$Ph_3SnOAl(L_5)_2$. The data obtained compared to the reported data in the literature and has the similarities, in which phenyl groups of Sn(IV) led in the equatorial plane, with average [C-Sn-C and C-Sn-C] angles of 109.1º to 107.6º and 113.10º to 103.4º, respectively having similarities.[32] One of phenyltinphenyl angles in $Ph_3SnOAl(OPr^i)L_5$ for Sn(IV) in concerned unit, Sn(25)-C(137)-C(161), 131.5º, and Sn(90)-C(91)-C-92), 124.9º, was significantly larger than the others, and both were larger than C-Sn-C angles in triphenyltin(IV). It seemed that carbonyl oxygen opened up carbon-tin-carbon angle nearest to it.

The process of determining energy minimization was repeated several times to find global minimum energy.[33]

Table 7. Bond Angles of $Ph_3SnOAl(L_5)_2$

S. No.	Geometrical sequencing of atoms	Bond Angle (°)	S. No.	Atoms numbering and their location	Bond Angle (°)
1.	C(26)-Sn(25)-C(38)	103.4	6.	Sn(25)-O(44)-Al(45)	104.7
2.	C(26)-Sn(25)-O(44)	104.7	7.	N(8)-Al(45)-O(18)	103.2
3.	C(32)-Sn(25)-C(38)	113.1	8.	N(8)-Al(45)-O(44)	105.8
4.	C(38)-Sn(25)-O(44)	139.3	9.	N(8)-Al(45)-N(53)	160.0
5.	N(8)-Al(45)-O(63)	109.9	10.	O(44)-Al(45)-O(63)	131.4

Molecular and solvent accessible surface models of Sn(IV) and Al(III) were designed and presented figure 3(a) and 3(b). MM force field calculations performed for molecular structure of $Ph_3SnOAl(OPr^i)L$ and $Ph_3SnOAl(L)_2$ showed that more favoured structures were formed by tridentate coordination of one ligand and a bidentate coordination of other.

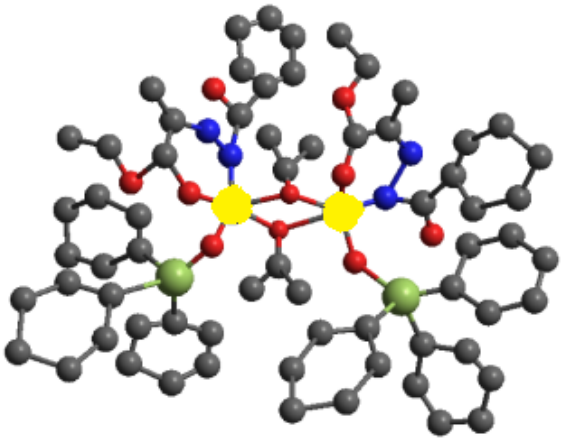

Figure. 3a. Molecular model of $Ph_3SnOAl(OPr^i)L_5$

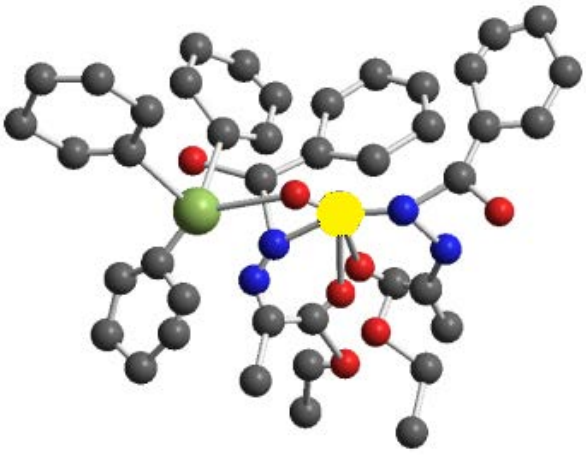

Figure. 3b. Molecular model of $Ph_3SnOAl(L_5)_2$

The tridentate chelation of both ligands was less favoured, their steric energy level was about 25-37% higher and this increase was probably not counterbalanced by bond energy of additional Al-O interaction. Among these species with tridentate-bidentate chelation, N(8)-Al, O(47)-Al and O(44)-Al coordination of tridentate ligand was energetically less favoured structure. Other possible binding namely e.g. O(45)-Al and O(46)-Al or N(74)-Al, O(109)-Al and O(63)-Al have fairly little energy differences and can be considered equally probable.[10,11,13] Accordingly, it was assumed that tridentate N(8)-Al, O(18)-Al and O(63)-Al coordination of one of ligand molecules and a bidentate N(8)-Al, and O(47)-Al coordination of other was the most favoured. This structure was as depicted in text.

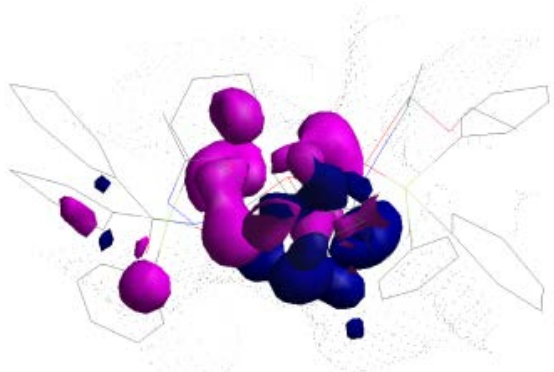

Figure. 4a. Molecular surface models of $Ph_3SnOAl(OPr^i)L_5$ with HOMO. Red regions in orbitals indicate the positive phase while blue present the negative phase.

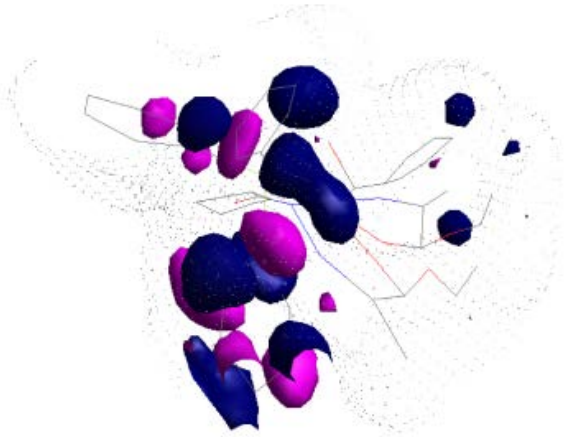

Figure. 4b. Molecular surface models of $Ph_3SnOAl(L_5)_2$ with HOMO. Red regions in orbitals indicate the positive phase while blue present the negative phase.

In both $Ph_3SnOAl(OPr^i)L$ and $Ph_3SnOAl(L)_2$ complexes, trimethyltin derivatives formed a polymeric structure with distorted tetrahedron geometry around Al(III) and their representative structures were given along with text. Here the

geometry around Sn(IV) was distorted tetrahedron. Four (O) and one (N) atoms were bonded to Al(III) at equatorial positions with essentially identical bond distances [mean Al-O = 2.230Å and Al-N = 2.118Å]. The Sn atom led 0.071 Å out of equatorial plane formed by three phenyl carbon towards more strongly bonded O. The C-Sn-O angle was approximately linear [108.2°] and the C-Sn-C angles were within expected range i.e. [C-Sn-C = 107.6° to 103.4° and O-Sn-C = 114.7 to 104.7°].

The bond distances of two N atoms with Al were 2.171 and 2.143 Å, too long to be strong covalent bonds. The N-Al-N linkage was not linear, having an angle of 160.0º, larger than value expected for a regular tetrahedron. The coordination geometry was best described as distorted tetragonal. Another important distortion was caused by asymmetric Al-O bond lengths. Therefore, O-Al-N angle of 103.2º was not consistent with true tetrahedral geometry, but instead was consistent with distorted tetragonal geometry. As a result, Al atom existed in a distorted tetragonal geometry in basal plane as defined by four -O- and one –N= within =N-N= backbone for $Ph_3SnOAl(OPr^i)L_5$.

The enthalpy change (DH) of $Ph_3SnOAl(OPr^i)L_5$ and $Ph_3SnOAl(L)_2$ was also calculated by using computational methods. DFT (Density Functional Theory) and MP2 (Second-order Møllere Plesset) were used. The difference between calculated and reported experimental enthalpy changes in gas state was compared. MP2 method underestimates enthalpy changes and DFT method overestimates them. DFT (B3LYP) method seems to be the best among the reported in experimental values. We also calculated enthalpy change in C_6H_6 solution using polarizable continuum method (PCM).

All calculations were carried out by using optimized geometries resulting from DFT calculations. The bulky phenyl groups of catalyst could strongly influenced reactivity of transition states by preventing coordination positions or by altering electronic structure of tin center. To distinguish steric and electronic factors of phenyl groups, different methods were widely used to study reaction mechanisms involving such factors. It was found both steric and electronic effects influenced transition states as well as initial and final metal complexes, and they changed reactivity in opposite manner: the steric effect introduced by PPh_3 ligands decreases activation barriers of rate determining step (from 32 kJ/mol to 21 kJ/mol), while electronic effects increased activation barriers (from19 kJ/mol to 31 kJ/mol). The steric repulsions should destabilize $Ph_3SnOAl(OPr^i)L_5$ and $Ph_3SnOAl(L)_2$, including in transition states, initial and final complexes.

The decrease of activation barrier suggests that initial and final complexes were more destabilized than transition states. However, electronic effects from PPh_3 ligands increased the barrier about 9 kJ/ mol. These calculations provided insight for developing new catalysts in future: different bulky ligands, which may provide same as the energy barriers associated with them, undoubtedly played critical roles in isomerization process. They were confirmed as the correct transition states first by intrinsic reaction coordinate calculations carried out by Gaussian 09. QM-PPh_3: full Quantum Mechanics (QM) calculations of whole system. In a full QM calculation, both steric and electronic effects from PPh_3 ligands were included. QM-PH_3: full Quantum Mechanics calculation of whole system, but PPh_3 ligands were modeled as PH_3 ligands. In this simplified model, neither steric nor electronic effects from PPh_3 ligands were included since all Ph_3 groups were replaced by H atom.

The results were very similar to gas phase calculations. Based on spectral and physiochemical analytical analysis (IR, ^{1}H NMR, ^{13}C NMR, ^{27}Al NMR, ^{119}Sn NMR and MS) analysis and molecular modeling, molecular structures of $Ph_3SnOAl(OPr^i)L_5$ and $Ph_3SnOAl(L)_2$ derived from L_1 to L_5 shown in figure 4(a) and 4(b) respectively.

6. Biological Activity

6.1 Antifungal activity

The antifungal activity of organotin i.e. $Ph_3SnOAl(OPr^i)L$ and $Ph_3SnOAl(L)_2$ using agar diffusion method were screened against different plant pathogens i.e. *Candida albicans, Aspergillus flavis and Candida glaberata*. Ketoconazole was used as standard drug and screening results presented graphically, in figure 5(a).

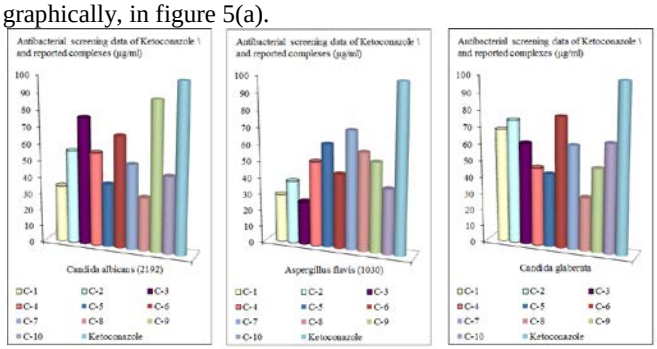

Figure. 5a. Antifungal activity of $Ph_3SnOAl(OPr^i)L$ and $Ph_3SnOAl(L)_2$

The assessment of fungal toxicity of complexes was based on (%) inhibition. Some of them exhibited quite significant activity, while compounds C-1 and C-8 were found to be less effective. But C-3 and C-9 exhibited very good inhibition against *Candida albicans*. Biological screening data of C-1, C-2 and C-3 against *aspergillus flavis* depicted low to moderate activity against fungi beside other complexes used with better physical properties. Antifungal activity of C-8 against *Candida glaberata* found very low. Further, it concluded that C-9, C-7 and C-6 were more active than other compounds and might act better antifungal agent. It was observed that C-1, C-2 and C-6 were more active against *Candida glaberata* comparatively other complexes. It was also noted that $Ph_3SnOAl(OPr^i)L$ with more phenyl groups showed greater inhibitory effect on one or

more types of fungus as compared to alkyl groups containing $Ph_3SnOAl(L)_{2)}$.[35]

The hydrogen of phenolic groups was so reactive that it enabled antioxidant to combine with constituents of living tissues, thus toxicity of Schiff base was due to alcoholic group. The presence of phenyl groups in compounds C-3, C-6 and C-9 bonded with tin atom was responsible for the rise in toxicity.

6.2 Antibacterial activity

Synthesized compounds showed significant antibacterial activity against *Escherichia coli, Bacillus subtilis, and Pseudomonas aeruginosa*. Imipenum was used as standard drug and showed more significant antibacterial activity as compared to C-4 against *Escherichia coli*, C-1 and C-2 against *Bacillus subtilis* and C-3 against *Pseudomonas aeruginosa*. The screening results were presented graphically in figure. 5(b).

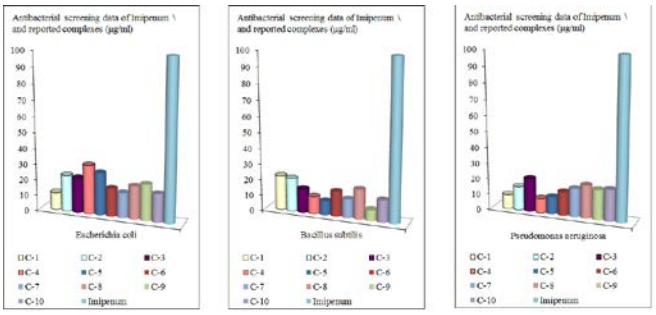

Figure. 5b. Antibacterial activity of $Ph_3SnOAl(OPr^i)L$ and $Ph_3SnOAl(L)_2$

As indicated in presented graphs, some of complexes i.e. C-1, C-4 and C-5 showed low antibacterial activity compared to others. C-2 and C-4 of $Ph_3SnOAl(L)_2$ showed fairly good activity against *Escherichia coli* and C-1 and C-2 against *Bacillus subtilis*, and C-3 and C-8 against *Pseudomonas aeruginosa*, but not as comparable as reference drugs. These results indicated that at the same concentrations, C-4 of $Ph_3SnOAl(L)_2$ has wider activity range than other complexes. *Escherichia coli, Bacillus subtilis*, and *Pseudomonas aeruginosa* as a bacterium resistance to most of antibiotics showed very poor sensitivity to both the series of the derivatives.[36]

C-1, C-4 and C-9 showed very less antibacterial activity among all complexes and activity of C-9 remained lower against *Bacillus subtilis* than other complexes. $Ph_3SnOAl(OPr^i)L$ with more phenyl groups showed greater inhibitory effect on one or more types of bacteria as compared to alkyl groups compounds $Ph_3SnOAl(L)_2$.[37-39]

The interaction of Al-moiety with rest of complex and microorganism was also reflected by DNA binding, wherein metal-free organic moieties does not bind DNA, whereas various metal complexes of metallocomplexes do. Sn(V)−OMCs was further demonstrated to bind and oxidative cleave DNA under reduction conditions in the air. The binding of Al-moiety to OMCs, and the significant oxidative activity of Sn(V)-OMCs provided further insights into bioactivity of metallocomplexes and Sn−oxygen and Al−oxygen chemistry. From these results it was apparent that attempting to introduce functionality of Al(III), the groups resulted in significant increased antibacterial and antifungal activity was due to its electron accepting characteristic and provided stability to bridge oxygen.

CONCLUSION

The formulation of triphenyl Sn(IV)-A(lII)-µ-oxoisopropoxide derivatives featuring different (*NOONO* and *OONO*) backbones was achieved by reaction of triphenyltin acetate and aluminium isopropoxide with corresponding ligand (L_1 to L_5) in presence of xylene. The chelating binding modes were observed by various modern spectral techniques (IR, ^{1}H NMR, ^{13}C NMR, ^{27}Al NMR, ^{119}Sn NMR and MS) and found in accordance with substituents (i.e. metal centres) attached to -N= and -O- atoms of *NOONO* and *OONO* backbones. Results obtained from spectral analysis revealed that steric constraints did not govern coordination modes entirely. Through reaction stoichiometry, a variety of coordination compounds featuring monodentate and µ-bridging coordination were observed. The monomeric complexes and aluminium were adducts, as previously seen with Al(III) due to their vacant orbital. However, µ-bridging and cluster types of complexes were likely lacking of steric effect on protection on -O- of *ONO* backbone.

The ^{1}H and ^{13}C chemical shift assignment, of the phenyltin moiety is straightforward from the multiplicity patterns, resonance intensities and also by comparing their nJ(^{13}C-$^{119/117}$Sn) values. The spin-spin coupling of 57 Hz between azomethine proton and tin nucleus, J(^{13}C-$^{119/117}$SnN=C^{1}H) was detected. The different analytical and mathematical analysis i.e. stability constant comparison, multinuclear NMR spectroscopy, ESI-MS and MM calculations provided enough information to suggest distorted tetragonal-pyramidal geometry may be most probable binding mode for compounds. Accordingly, in the bimetallic complexes, a tetra and pentadentate coordination modes of ligands was most probable in binding sites according to MM calculations.

Although five-coordinated Al(III) and four coordinated Sn(IV) of $Ph_3SnOAl(OPr^i)L$ and $Ph_3SnOAl(L)_2$, where coordination of –N= from imidazole moiety to Al(III) was described.[40-43] It was further shown that change in ratio of reactants i.e. $Ph_3SnOAl(OPr^i)L$ and $Ph_3SnOAl(L)_2$ has brought interesting differences in both series in reactivity and type of products formed having -µ- bridging.

This, -µ- bridging, opens up further opportunities for using these compounds as better microbial agents by exploiting their highly acidic nature of phenolic protons which influenced organotin(IV) bonding in moiety.[44,45] Especially with the role of -NH- groups involved in inter/intermolecular deprotonating or bonding to Al(III). Metals centre were capable of organizing

surrounding atoms to achieve pharmacophore geometries, not as correctly, rapidly and readily achieved by other means, figure 6(a) and 6(b). Additionally the effect of metals can be highly specific and modulated by recruiting cellular processes that recognize specific types of metal macromolecule interactions.

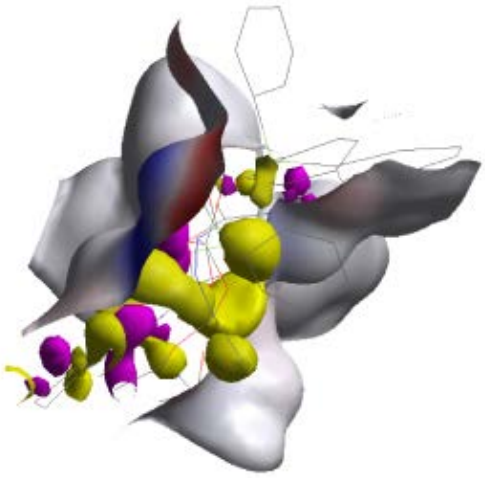

Figure. 6a. Metallopharmacomoleculular geometries of $Ph_3SnOAl(OPri)L$. The red diagram is from B3LYP calculations with PPh_3 ligands. White shades around the complex shows the microbial strains.

Understanding these interactions led the way towards rational design of metallopharmaceticals and implementation of new co-therapies. Metals might be useful in active site recognition and in bifunctional agents as secondary contacts to increase inhibitor affinity.

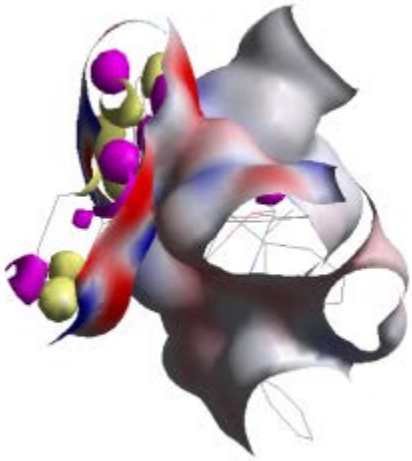

Figure. 6b. Metallopharmacomoleculular geometry of $Ph_3SnOAl(L)_2$. The red diagram is from B3LYP calculations with PPh_3 ligands. White shades around the complex shows the microbial strains.

The polarizability effect owes its existence because of excess charge on Sn and as a result of this, donor-acceptor interaction between molecule-biological target occurred. The presence or absence of certain effect was governed by different substituents in both the series of the complexes. In most cases the influence of substituents can be realistically explained only if polarizability effect was taken into consideration. The knowledge of substituent effects permit a better understanding of such factors and their influence on biological activity of organometallics.

ACKNOWLEDGEMENTS

One of the authors (Rajiv Kumar) gratefully acknowledges his younger brother Bitto for motivation. Authors acknowledge I.I.T. Bombay for recording ^{1}H and ^{13}C NMR spectra.

REFERENCES AND NOTES

1. Pietrzykowski, T. Skrok, S. Pasynkiewicz, M. Brzoska-Mizgalski, J. Zachara, R. Anulewicz-Ostrowska, K. Suwinska and L.B. Jerzykiewicz, Reactions of methyl- and ethylaluminum compounds with alkoxyalcohols. The influence of alkoxyalcohol substituents on the structure of the complexes formed, *Inorg. Chim. Acta.* **2002,** *334*, 385-394.
2. C.-H. Lin, B.-T. Ko, F.-C. Wang, C.-C. Lin and C.-Y. Kuo, Electronic and steric factors affecting the formation of four or five-coordinated aluminium complexes: syntheses and crystal structures of some aluminum alkoxides, *J. Organomet. Chem.* **1999,** *575*, 67-75.
3. H. Yi-Lun, K. Bor-Hunn, Bao-Tsan, L. Chu-Chieh, Reactions of amides with organoaluminium: a useful synthetic route to aluminium diketiminates, *J. Chem. Soc., Dalton Trans.* **2001,** 1359-1365.
4. D.A. Atwood and B.C. Yearwood, The future of aluminium chemistry, *J. Organomet. Chem.* **2000,** *600*, 186-197.
5. M. Gielen, P. Lelieveld, D. de Vos, R. Willem, Metal based antitumour drugs. Vol. 2, Freund, Tel Aviv, 29-54, 1992.
6. M. Gielen, E.R.T. Tiekink, Metallotherapeutic drugs and metal-based diagnostic agents: The use of metals in medicine, John Wiley & Sons, New York, 2005.
7. Ambrosini, E. Bertoli, G. Zolese, F. Tanfani, Interaction of tributylin acetate and tributyltin chloride with dipalmitoyl phosphatidylcholine model membrane. *Chem. Phys. Lipids.* **1991,** 59, 189-197.
8. R.M. Fernandes, E.S. Lang, E.M.V. Lopez and G.F. Desousa, Organotin(IV) complexes of 4,6-dimethylpyrimidine-2-thione,Me_2PymtH. Preparation, characterization and crystal structure determination of cis-[$Ph_2Sn(Me_2Pymt)_2$] and [$Ph_3Sn(Me_2Pymt)$], *Polyhedron*, **2002,** *6*, 1149-1153.
9. S.J. Obrey, S.G. Bott, A.R. Barron, A lewis base promoted alkyl/alkoxide ligand redistribution: reaction of [$Me_2Al(m\text{-}OCPh_3)]_2$ with THF, *Organometallics*, **2001,** *20*, 5119-5124.
10. M. Gielen. Tin-based antitumour drugs, *Coord. Chem. Reviews*, **1996**, 151, 41-51.
11. O. Koper, I. Lagadic, K.J. Klabunde, Destructive adsorption of chlorinated hydrocarbons on ultrafine (Nanoscale) particles of calcium oxide. 2. *Chem. Mater*, **1997,** 9, 838-842.
12. J. Devi, R. Kumar, Synthesis, spectral and thermal studies on schiff base derivatives of heterobimetallic [Ca(II)-Ti(IV)]-μ-oxoisopropoxide, *Chem. Sci. Trans.*, **2013,** 2(4), 1214-1221.
13. (a) A.I. Vogel, A text book of quantitative analysis, Longman: London; 1989. (b) D.D. Perrin, W.L.F. Armarego, D.R. Perrin. Purification of laboratory chemicals, 2nd ed., Pergamon Press: New York; 1980.
14. E. Clementi, G. Corongiu. (Eds) Methods and techniques in computational chemistry: METECC-95, STEF, Cagliari, 1995;

15. M. Sharma, A. Singh, R.C. Mehrotra. Synthesis and characterization of homo- and heterobimetallic diethanolaminates of alkaline earth metals. *Polyhedron*, **2000,** 19, 77-83. [Symptoms such as wheezing, cough, chest pain and dyspnoea on exertion reported in workers handling $SnCl_4$ were probably due to elevated levels of hydrogen chloride formed by the combination of SnCl4 and water in the presence of heat]
16. K. Nakamoto. Infrared and raman rpectra of inorganic and coordination compounds, John Wiley and Sons, New York, 1986.
17. M.B. Jones, C.E. MacBeth, Tripodal phenylamine-based ligands and their Co^{II} complexes Matthew B. Jones and Cora E. Mac Beth, *Inorg. Chem.* **2007**, *46*, 8117-8119.
18. G. Sébastien, A. Sabrina, R. Patrice, P. Stéphane, D. Jean-Rogers, D. Michel, A spectroscopic investigation of the complexing ability of catecholate or salicylate derivatives towards aluminium(III), *Polyhedron*, **2004**, *23*, 2393-2404.
19. L.J. Bellamy. The infrared spectra of complex molecules, Chapman and Hall, London, Reprinted, 1978.
20. N.B. Colthup. L.H. Daly, S.E. Wiberly. Introduction to infrared and raman spectroscopy, Academic Press, New York, 1990.
21. S. Giroux, P. Rubini, B. Henry, S. Aury, Complexes of praseodymium(III) with D -gluconic acid, *Polyhedron*, **2000**, *19*, 1567-1574.
22. E. Breitmaier, W. Voelter. Carbon-13 NMR spectroscopy: High-resolution methods and applications in organic chemistry and biochemistry, John Wiley & Sons; 3 edition, 1986.
23. D. Doddrell, I. Burfitt, W. Kitching, M. Bullpitt, L. Che-Hung, R.J. Mynott, J.L. Considine, H.G. Kuivila, R.H. Sarma. Carbon-13 Fourier transform NMR study of the organotin compounds. II. Karplus-type dependence of vicinal tin-119-carbon-13 coupling *J. Am. Chem. Soc.*, **1974**, *96*, 1640-1642
24. Lyčka, D. Micák, j. Holeček, M. Biesemans, J.C. Martins, R. Willem. ^{13}C-^{119}Sn Correlation NMR in Solution and Solid-State CP/MAS NMR of Bis(tributylstannyl(IV)) O-5,6-Isopropylidene-l-(+)-ascorbate, *Organometallics*, **2000**, *19*, 703-706.
25. S. Shaukat, R. Zia-ur, M. Niaz, S. Afzal, A. Saqib, K. Nasir, M. Auke. Bioactive hepta- and penta-coordinated supramolecular diorgano tin(IV) Schiff bases, *J. of Organomet. Chem.*, **2013**, *741*, 59-66.
26. G. Shadab, M. Majid, T. Shahram, M. Valiollah, B. Iraj Mohammad poor, B. Behjat, S. Faranak. High-valent tin(IV) porphyrins: Efficient and selective catalysts for cyclopropanation of styrene derivatives with EDA under mild conditions, J. of Organomet. Chem. **2013,** *741*, 78-82.
27. T. Jan, K. Hana, P. Zdenka, R. Ales. Preparation and structure of tin(IV) catecholates by reactions of C,N-chelated tin(IV) compounds with a catechol or lithium catecholate, and various stannylenes with a quinone, J. of Organomet. Chem. **2013**, *745*, 25-33
28. R. Benn, A. Rufinska, H. Lehmkul, E. Janssen, C. Kruger. ^{27}Al-NMR spectroscopy: a probe for three-, four-, five-, and six-fold coordinated Al atoms in organoaluminum Compoundsc. *Angew. Chem. Int. Ed. Engl.* **1983**, *22*, 779-780.
29. M. Pellei, G.G. Lobbia, M. Ricciutelli, C. Santini. Synthesis and spectroscopic characterization of new organotin(IV) complexes with bis(3,5-dimethylpyrazol-1- yl)dithioacetate. *J. Coord. Chem.* **2005**, *58*, 409-420.
30. A.A. Abou-Hussen, N.M. EL-Metwally, E.M. Saad, A.A. EL-Asmy, Spectral, magnetic, thermal and electrochemical studies on phthaloyl bis(thiosemicarbazide) complexes. *J.of Coord. Chem.* **2005**, *58*, 1735-1749
31. H. Chin, B.R. Penfold. Crystal and molecular structures of two polymeric organotin carboxylates, $C_{15}H_{12}O_2Sn$, $C_5H_9F_3O_2Sn$. J. Crystal Mol. Struct. **1973**, *3*, 285-297.
32. K. Wakamatsu, A. Orita, J. Otera. Evaluation of tin-oxygen bond association by means of ab initio molecular orbital calculations. *Organometallics*, **2008**, *27*, 1092-1097
33. F.M. Bickelhaupt, E.J. Baerends, K.B. Lipkowitz, D.B. Boyd. *Reviews in Computational Chemistry*, Wiley-VCH, New York, **2000**, *15*, 1-86.
34. Rahman, M.I. Choudhary. Thomsen, W.J. Bioassay techniques for drug development, Harwood Academic Press, Amsterdam 2001.
35. M.M. Pour, V. Špulák, J. Balšánek, V. Kuneš, B. Waisser. 3-Phenyl-5-methyl-2H,5H-furan-2-ones: tuning antifungal activity by varying substituents on the phenyl ring. *Bioorg. Med. Chem. Lett.*, **2000,** *10*, 1893-1901.
36. R.D. Pearson, A.A. Manian, D. Hall, J.L. Harcus. Antileishmanial activity of chlorpromazine. *Antimic. Ag. Chemo.* **1984**, *25*, 571-574.
37. W. Rehman, K.B. Musa, B. Amin. Comparative study of structure: activity relationship of di and triorganotin (IV) complexes of monomethyl glutarate. *J. Braz. Chem. Soc.* **2005**, *16*, 827-834.
38. F.M. Morad, M.M. Ajaily, S.B. Gweirif. Preparation, physical characterization and antibacterial activity of Ni(II) schiff base complex. *J. of Science and Its Applications*, **2007,** *1*, 72-78.
39. P. Spigaglia, F. Barbanti, P. Mastrantonio. Detection of a genetic linkage between genes coding for resistance to tetracycline and erythromycin in Clostridium difficile. *Microb. Drug Resist.* **2007,** *13*, 90-95.
40. Xiong-Bin, Y. Qiong, W. Qian, S. Yu-Mei, X. Ren-Gen, Y. Xiao-Zeng. The first organometallic carbonyl tungsten complex of antibacterial drug norfloxacin. *Inorg. Chem. Commun.* **2004,** *7*, 1302-1305.
41. Y. Wang, G.R. Wang, A. Shelby, N.B. Shoemaker, A.A. Salyers. A newly discovered *bacteroides* conjugative transposon, CTnGERM1, Contains genes also found in gram-positive bacteria. *Appl. Environ. Microbiol.* **2003,** *69*, 4595-4603.
42. B.S. Chhikara, A.K. Mishra, V. Tandon. Synthesis of bgifunctional chelating agents to label monoclonal antibodies for radioimmunodiagnosis of cancer. *Int. Arch. Sci. Technol.,* **2006,** 6(1), 5-9.
43. R. Johar, R. Kumar, A.K. Aggarwal. Tailoring methodologies for the architecture of organometallic frameworks of Bi(V) derived from antibiotics: Spectral, MS, XRPD and molecular modeling with antifungal effectiveness. *J Integr Sci Technol*, **2013,** 1(1), 54-64.
44. Pauling, L. Nature of the chemical bond", Cornel University Press, 2nd. Ed, Cornell, New York, USA (1947) 251.
45. Nugent, W.A.; Mayer, J.M. Metal-ligand multiple bonds, Wiley Interscience, New York, USA (1988).